Experimental realization of one-dimensional optical quantum walks*

Xue Peng(薛 鹏)[a)b)†], Qin Hao(秦 豪)[a)], Tang Bao(唐 宝)[a)],
Zhan Xiang(詹 翔)[a)], Bian Zhi-Hao(边志浩)[a)], and Li Jian(李 剑)[a)]

[a)] *Department of Physics, Southeast University, Nanjing* 211189, *China*
[b)] *State Key Laboratory of Precision Spectroscopy, East China Normal University, Shanghai* 200062, *China*

(Received 22 April 2014; revised manuscript received 28 May 2014; published online 24 September 2014)

We analyze the process of a discrete-time quantum walk over 4 steps and 5 positions with linear optics elements. The quantum walk is characterized by a ballistic spread of wavepackets along 4 steps. By employing different initial coin states, we observe non-Gaussian distribution of the walkers' finial position, which characterizes a quadratic enhancement of the spread of photon wavepackets compared to a classical random walk. By introducing controllable decoherence, we observe the quantum-to-classical transmission in a quantum walk architecture.

Keywords: quantum walk, quantum-to-classical transmission, decoherence

PACS: 03.67.Mn, 03.65.Ta, 05.40.Fb, 03.67.Ac **DOI:** 10.1088/1674-1056/23/11/110307

1. Introduction

Quantum walks (QWs) were introduced in 1990s and they exhibit distinct features compared to classical random walks (RWs).[1] Hence, QWs can be used to develop quantum algorithms[2–5] and to study quantum effects, such as the Anderson localization effect,[6–9] topological phases[10] and energy transport in photosynthesis.[11] For the last two decades, QWs have been demonstrated experimentally using energy levels in nuclear magnetic resonance,[12] phase and position space of trapped ions,[13–15] trapped neutron atoms,[16] the frequency space of an optical resonator,[17] photons in beam splitter array, in a fiber loop, and in waveguide structures.[18–25]

In this paper, we present an experimental realization of photonic QWs in space. We investigate the evolution of photons moving in a discrete environment presenting controllable decoherence. Due to the intrinsically stable interferometers used in our experiment, our approach is robust and is able to introduce and control decoherence. In our experiment, we realize the QW of photons by employing a linear optical network and a controlled amount of decoherence to explore the quantum-to-classical transition.

2. Experiment and results

Before we proceed with our experiment on QW, let us recall the standard model of a one-dimensional (1D) discrete-time QW, which consists of a quantum walker carrying a quantum coin. The coin is flipped before each step and the walker takes steps according to the outcomes of the coin toss. An arbitrary unitary operation C in SU(2) can be used as coin toss, followed by a conditional position shift operation $S = \sum_x |x+c\rangle\langle x| \otimes |c\rangle\langle c|$ with $c = \pm 1$ representing two sides of the coin. The evolution of the walker+coin system is given by a unitary operation $U = S(I \otimes C)$ and the initial state $|\varphi(0)\rangle$ evolves in time t according to $|\varphi(t)\rangle = U^t|\varphi(0)\rangle$.

The position variance of the walker $\sigma^2 = \langle x^2\rangle - \langle x\rangle^2$ is linear on the number of steps N for RWs. Whereas, the variance of QWs grows quadratically with N and the position distribution shows a ballistic diffusion compared to that of RWs. With decoherence the spreading of a QW is transmitted from a ballistic to diffusive scaling, and with quantumness losing the QW is transmitted to RW.[26–31]

A straightforward implementation of an optical QW is realized with multiple beam splitters (BSs) and phase shifters.[17] However, this increases the experimental complexity because it is difficult to achieve high optical stability and exact alignments of BSs. In our experiment, to solve the obstacle we instead use birefringent calcite beam displacers (BDs) to build interferometers. The optical axis of each calcite prism is cut so that vertically polarized light is directly transmitted and horizontal light undergoes a lateral displacement into a neighboring mode, which will interfere with the vertical light in the same mode.

We generate the input photons with a pulsed laser (Ti: sapphire laser systems) with a central wavelength of 800 nm, a pulse width of 150 fs, and a repetition rate of 76 MHz. The input power is typically 1.7 mW, resulting in an output power of tens to hundreds μW at the power meter. Although the experiment has been performed using a coherent source rather than single photons, it is sufficient for describing single-photon be-

*Project supported by the National Natural Science Foundation of China (Grant Nos. 11174052 and 11474049), the National Basic Research Development Program of China (Grant No. 2011CB921203), and the Open Fund from the State Key Laboratory of Precision Spectroscopy of East China Normal University, China.
†Corresponding author. E-mail: gnep.eux@gmail.com
© 2014 Chinese Physical Society and IOP Publishing Ltd

haviour in QWs as it has been proven in Refs. [17] and [32]–[34]. The experimental realization of QWs depends on the interference of the probability amplitudes of wavepackets, while the behavior of QWs is not influenced by the statistic property of photons. Hence, we can realize a photonic QW with coherent light instead of a true single photon source. Compared to the previous realization of a QW with single photons,[21] our protocol is easier to be realized experimentally by releasing the requirement of a true single photon source.

The coin state is encoded in the polarization $|H\rangle$ and $|V\rangle$ of the input photon. Using a quarter- and half-wave plates (QWPs and HWPs), the initial coin states are set to $|c(\theta,\chi)\rangle = \cos(\theta/2)|H\rangle + e^{i\chi}\sin(\theta/2)|V\rangle$ with $\theta \in [0,\pi]$ and $\chi \in [0,2\pi)$, leading to symmetric or asymmetric probability distributions. In the basis $\{|H\rangle,|V\rangle\}$, the coin flipping operation for each step is given by

$$C(\vartheta) = \begin{pmatrix} \cos(2\vartheta) & \sin(2\vartheta) \\ \sin(2\vartheta) & -\cos(2\vartheta) \end{pmatrix},$$

with $\vartheta \in (0,\pi/4)$, consisting of a polarization rotation, which is realized with a HWP setting. For example, the Hadamard operator is realized with a HWP set to $\vartheta = 22.5^\circ$.

The positions of the walker are represented by longitudinal spatial modes. The unitary operator for each step

$$U = \sum_x (|x+1\rangle\langle x| \otimes |H\rangle\langle H| + |x-1\rangle\langle x| \otimes |V\rangle\langle V|)\,(\mathbf{1}\otimes C(\vartheta)),$$

with the position shift operator acting on these modes, is implemented by a BD with length 28 mm and clear aperture 10 mm × 10 mm. The optical axis of each calcite prism is cut so that vertically polarized light is directly transmitted and horizontal light undergoes a 2.7-mm lateral displacement into a neighboring mode, which will interfere with the vertical light in the same mode. Each pair of BDs forms an interferometer. Since the probability of the walker appearing in other sites is zero, only odd sites of the walker are labeled at each odd step, while at each even step only even sites are labeled.

The 4 steps of a QW are shown in detail in Fig. 1. The longitudinal spatial modes after the 1st step are recombined interferometrically at the 2nd step. The interference visibility reaches 0.9985 per step. Phase shifters are used to compensate the phase shifts due to the imperfect surface of the BDs. The photons emerge in the $N+1$ spatial modes at the output of an N step and are subsequently detected by a power meter. Due to the size of the BDs, the light of the lowest spatial mode leaks out from the 4th BD and can still be detected by laterally moving the BD via a power meter. The experimentally measured probabilities and the theoretical predictions for 1 to 4 steps of a standard Hadamard QW are shown in Fig. 2. The probabilities are obtained by the normalizing light intensity at each position to the total intensities for the respective step. The experimental data are in excellent agreement with the theory, with an average distance $d = \left(\sum_x \left|P^{\rm exp}(x) - P^{\rm th}(x)\right|\right)/2$, of 0.018 for the standard Hadamard QW and 0.013 for the simulated RW (a fully decohered QW). For the asymmetric initial coin state $|H\rangle$, the final state of the walker after 3 steps clearly shows non-Gaussian distribution, while it shows the characteristic shape of a standard Hadamard QW for the symmetric initial coin state $(|H\rangle + i|V\rangle)/\sqrt{2}$ only after 4 steps: two pronounced side peaks (measured as 0.367 ± 0.015 and 0.360 ± 0.011, theoretical simulated as 0.375) and the low probability (measured as 0.151 ± 0.009, theoretical simulated as 0.125) in the original position of the walker shown in Fig. 3(a). For large steps, the relative phase shifts between the neighboring BDs caused by the nonplanar optical surfaces might lead to decoherence and have a significant impact on QWs, as shown in Fig. 3(b).

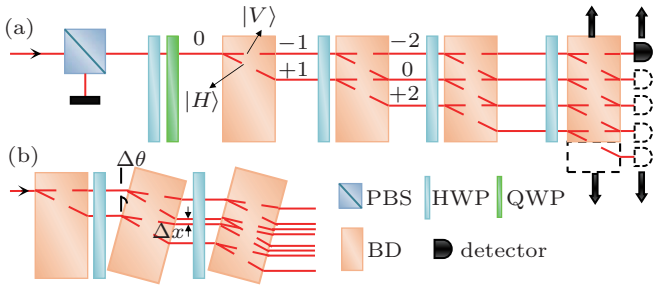


Fig. 1. (color online) Experimental schematic diagram. (a) Detailed sketch of the setup for the first 4 steps of QW. A laser field is coupled to the optical network. Arbitrary initial coin states are prepared by the polarizing beam splitter (PBS) and wave plates. Due to the size of the beam displacers (BDs), the light of the lowest spatial mode leaks out from the 4th BD and can still be detected by laterally moving the BD via a power meter. (b) A relative angle $\Delta\theta$ between two BDs reduces the recombined photon's spatial mode overlap, which introduces controllable dephasing.

The controllable decoherence, such as dephasing, can transmit QWs to RWs. A non-zero relative angle between neighboring BDs leads to both a temporal delay and a transversal mode mismatch between the interfering wavepackets, which cause the dephasing that is shown in Fig. 1. The dephasing can be tuned by adjusting relative angle values. The interference visibility at each step reduces to 0 for the relative angle of $\Delta\theta = 10.375^\circ$ and $\Delta x = 2.7\ (1/\cos\Delta\theta - 1) = 0.0449$ mm, and the QW is transited to RW completely. Figure 3(b) shows the experimentally measured probability distribution of a fully decohered QW at the 4th step, compared to theory. From the experimental data of the normalized variance σ^2/N, we observe a ballistic spread for a standard Hadamard QW and diffusive spread for a fully decohered QW in Fig. 4.

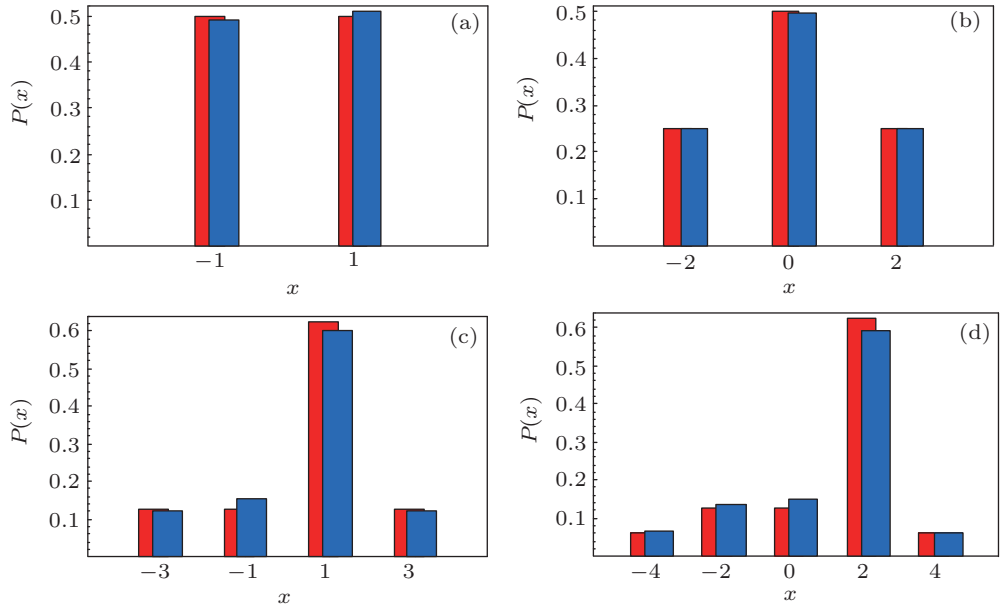


Fig. 2. (color online) Experimentally measured and numerically simulated probability distributions for successive steps of the Hadamard QW with the asymmetric initial coin state $|H\rangle$ up to 4 steps ((a)–(d) the first, second, third and fourth steps, respectively). The blue bars show experimental data and the red bars show theoretical predictions.

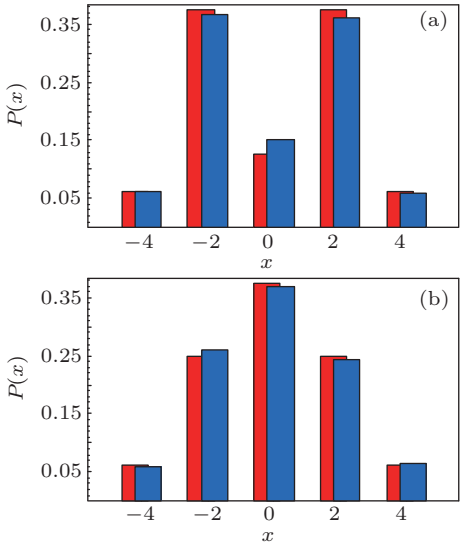


Fig. 3. (color online) Experimental data of probability distributions for successive steps of the standard Hadamard QW (a) and a fully decohered QW (b) with the symmetric initial coin state $(|H\rangle + |V\rangle)/\sqrt{2}$ up to 4 steps, with respective theoretical simulation. The blue bars (right bars) show experimental data and the red bars (left bars) show theoretical predictions.

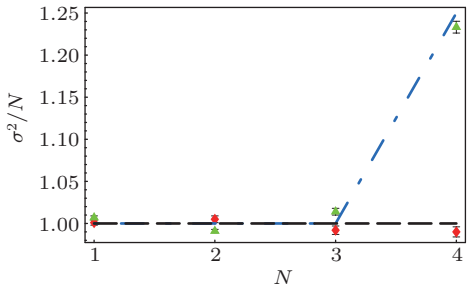


Fig. 4. (color online) Measured and simulated normalized position variances for a Hadamard QW (green triangles) and a fully decohered QW (red diamonds) for 1 to 4 steps, with respective theoretical simulation (blue and black lines). The error bars are due to photon statistics and some of them are smaller than the symbol size.

3. Conclusion

In conclusion, we implement a stable and efficient way to realize QWs embedded in a broader framework and show that the decoherence can influence the evolution of wavepackets. The standard Hadamard QW spreads ballistically and the fully decohered QW spreads diffusively. In contrast to previous experiments, we benefit from the high stability and full control of both coin and walker at each step and at each given position. Further work could implement QWs with a walker in two-dimensional lattice, in which richer choices of defects, such as string defects, would help us to study the topology of QWs and develop applications, such as quantum transport problems.

References

[1] Aharonov Y, Davidovich L and Zagury N 1993 *Phys. Rev. A* **48** 1687
[2] Ambainis A 2003 *International Journal of Quantum Information* **1** 507
[3] Childs A M, Cleve R, Deotto E, Farhi E, Gutmann S and Spielman D A *Proc. 35th ACM Symposium on Theory of Computing (STOC* 2003*)* 59
[4] Shenvi N, Kempe J and Whaley K B 2003 *Phys. Rev. A* **67** 052307
[5] Kempe J 2003 *Contemporary Physics* **44** 307
[6] Anderson P W 1958 *Phys. Rev.* **109** 1492
[7] Brun T A, Carteret H A and Ambainis A 2003 *Phys. Rev. Lett.* **91** 130602
[8] Zhang R, Xue P and Twamley J 2014 *Phys. Rev. A* **89** 042317
[9] Zhang R, Qin H, Tang B and Xue P 2013 *Chin. Phys. B* **22** 110312
[10] Kitagawa T, Rudner M S, Berg E and Demler E 2010 *Phys. Rev. A* **82** 033429
[11] Oliveira A C, Portugal R and Donangelo R 2006 *Phys. Rev. A* **74** 012312
[12] Du J, Li H, Xu X, Shi M, Wu J, Zhou X and Han R 2003 *Phys. Rev. A* **67** 042316
[13] Zähringer F, Kirchmair G, Gerritsma R, Solano E, Blatt R and Roos C F 2010 *Phys. Rev. Lett.* **104** 100503
[14] Schmitz H, Matjeschk R, Schneider C, Glueckert J, Enderlein M, Huber T and Schaetz T 2009 *Phys. Rev. Lett.* **103** 090504

[15] Karski M, Forster L, Choi J M, Steffen A, Alt W, Meschede D and Widera A 2009 *Science* **325** 174
[16] Cote R, Russell A, Eyler E E and Gould P L 2006 *New J. Phys.* **8** 156
[17] Bouwmeester D, Marzoli I, Karman W, Schleich G P and Woerdman J P 1999 *Phys. Rev. A* **61** 013410
[18] Peruzzo A, Lobino M, Matthews J C F, Matsuda N, Politi A, Poulios K, Zhou X, Lahini Y, Ismail N, Worhoff K, Bromberg Y, Silberberg Y, Thompson M G and O'Brien J L 2010 *Science* **329** 1500
[19] Perets H B, Lahini Y, Pozzi F, Sorel M, Morandotti R and Silberberg Y 2008 *Phys. Rev. Lett.* **100** 170506
[20] Schreiber A, Gábris A, Rohde P P, Laiho K, Štefaňák M, Potoček V, Hamilton C, Jex I and Silberhorn Ch 2010 *Science* **336** 55
[21] Broome M A, Fedrizzi A, Lanyon B P, Kassal I, Aspuru-Guzik A and White A G 2010 *Phys. Rev. Lett.* **104** 153602
[22] Schreiber A, Cassemiro K N, Potoček V, Gábris A, Mosley P J, Andersson E, Jex I, Silberhorn Ch 2010 *Phys. Rev. Lett.* **104** 050502
[23] Sansoni L, Sciarrino F, Vallone G, Mataloni P, Crespi A, Ramponi R and Osellame R 2012 *Phys. Rev. Lett.* **108** 010502
[24] Xue P, Qin H, Tang B and Sanders B C 2014 *New J. Phys.* **16** 053009
[25] Xue P, Qin H and Tang B 2014 *Sci. Rep.* **4** 4825
[26] Xue P and Sanders B C 2008 *New J. Phys.* **10** 053025
[27] Xue P, Sanders B C and Leibfried D 2009 *Phys. Rev. Lett.* **103** 183602
[28] Xue P, Sanders B C, Blais A and Lalumiére K 2008 *Phys. Rev. A* **78** 042334
[29] Xue P and Zhang Y S 2013 *Chin. Phys. B* **22** 070302
[30] Xue P 2013 *J. Comput. Theor. Nanosci.* **10** 1606
[31] Qin H and Xue P 2013 *Chin. Phys. B* **23** 010301
[32] Mosley P J, Croke S, Walmsley I A, Barnett S M 2006 *Phys. Rev. Lett.* **97** 193601
[33] Do B, Stohler M L, Balasubramanian S, Elliott D S, Eash C, Fischbach E, Fischbach M A, Mills A and Zwickl B 2005 *J. Opt. Soc. Am. B* **22** 499
[34] Zhang P, Ren X F, Zou X B, Liu B H, Huang Y F and Guo G C 2007 *Phys. Rev. A* **75** 052310